

2D Hall Arrays for High Resolution Tokamak Magnetic Field Imaging

Samuel Shelton[✉] and Will Midgley[✉]

This is an early draft as is subject for change. Its primarily here to get the extra figures out to audiences that are attending SOFE2025. Please do not distribute. Many changes will be made for/if this is submitted anywhere.

Abstract—This paper presents the use of a two-dimensional array of magnetic field sensors designed to image the magnetic field produced in the vacuum vessel of the upcoming SOUTH tokamak. Designed to de-risk engineering efforts by allowing for precise mapping of toroidal and null field configurations within the plasma boundary region, this represents the first use of such a device within the context of fusion. Using low-noise circuitry and multiple analogue-to-digital converters in parallel, the device can achieve up to 20 kHz of analogue bandwidth across 256 sensors, with an effective sensitivity of 0.32 mT against a dynamic range exceeding ± 150 mT. The device can also be operating in a real-time mode using a micro-controller, allowing interactive visualizations of magnetic fields for outreach and pedagogical purposes. Preliminary imagery and simulated reconstructions are presented, with the device anticipated to assist with the research and development, manufacturing and commissioning of the SOUTH tokamak over the next 12–18 months.

Index Terms—tokamak, diagnostics, instrumentation, magneto-vision, Hall effect

I. INTRODUCTION

THE SOUTH Tokamak (shown in Figure 1) is being developed at the University of New South Wales in Sydney, Australia as a student project called *AtomCraft* [1]. SOUTH — the Student Operated Undergraduate Tokamak with rf Heating — will be the first tokamak designed and built entirely by undergraduates. It will be a compact, spherical tokamak employing conventional magnets and utilizing a combination of ohmic heating and electron cyclotron resonance heating (ECRH). The design is influenced primarily by the Danish NØTH tokamak [2] and its predecessor, Tokamak Energy’s ST-25 [3], with cool and power supply designs inspired by SMART [4].

SOUTH is expected to operate with a toroidal on-axis magnetic field of 100 mT and a 100 ms pulse; the device has a major radius of approximately 0.3 m, with a vacuum vessel diameter of 30 cm. Initial plasma operations and anticipated to commence in late 2026, with plasma currents of 3 kA and

S. Shelton and W. Midley are with the School of Mechanical and Manufacturing Engineering, UNSW Sydney, and the SOUTH collaboration.

Presentation of this work at SOFE2025 was funded by the Sir William Tyree foundation through the UNSW Nuclear Innovation Center (UNIC) Travel Award.

Corresponding author S. Shelton, s.shelton@unsw.edu.au.

Manuscript received Month XX, 202X; revised Month XX, 20XX.

Supporting videos for the content in this paper are available at <https://doi.org/XX.XXX/TPS.202X.XXXXXXXX>

Digital Object Identifier XX.XXX/TPS.202X.XXXXXXXX

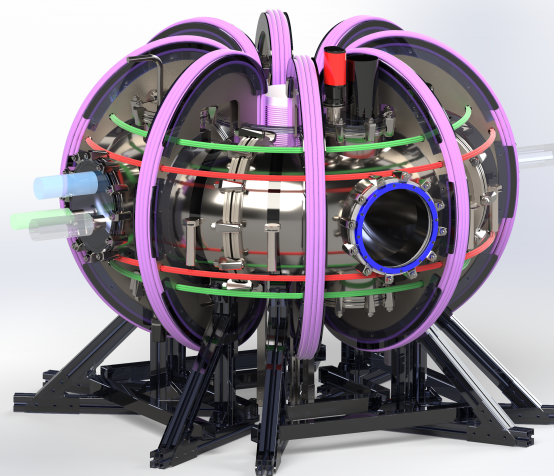


Fig. 1. Preliminary render of SOUTH tokamak with placeholder instrumentation, vacuum system, fueling, and RF equipment

plasma temperatures of about 10 eV expected [1]. *AtomCraft*’s primary focus is pedagogical, providing students with hands-on experience in fusion engineering from as early as their second undergraduate year.

As a student budget, *AtomCraft* operates under strict budgetary constraints, with a strong emphasis on safety and risk management. External funding is sourced from philanthropic institutions and commercial fusion organizations, necessitating clear and communicable results for outreach. The idea of a two-dimensional Hall array emerged as a tool to detect technical issues with the magnet system prior to plasma operation, with potential as an outreach and recruitment tool due to its visual and interactive nature.

A. Hall sensors and magnetic arrays in Fusion

Hall effect sensors are widely used in fusion engineering for magnetic field monitoring, plasma diagnostics [5], [6], and current sensing [7]. Low-density arrays have an established use in magnetic field mapping [8], and a high-density one-dimensional array of Hall sensors has been demonstrated as an effective tool for measuring both vacuum and plasma-generated poloidal magnetic fields in magnetically confined plasmas [9].

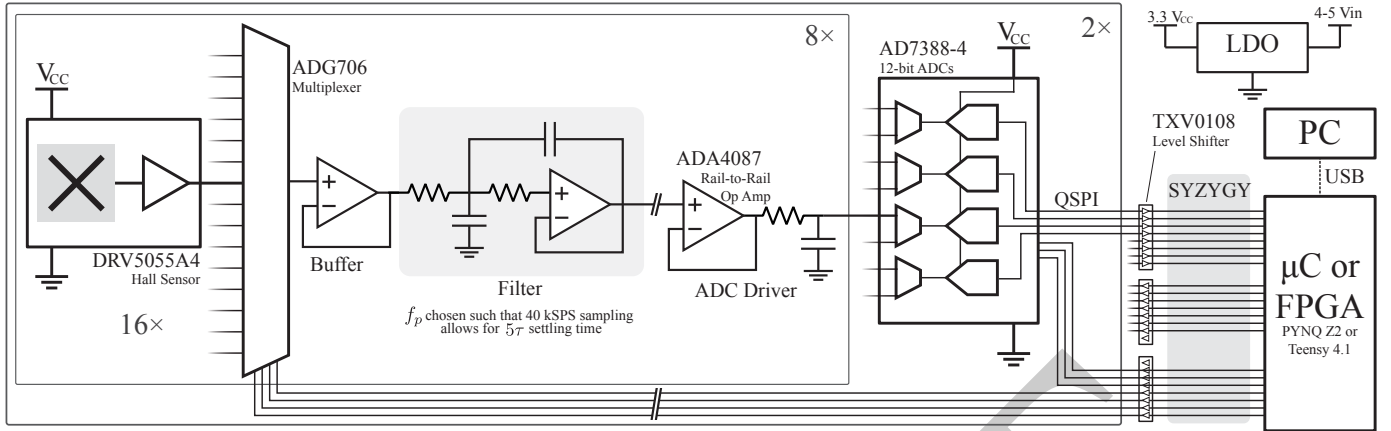


Fig. 2. Simplified circuit schematic showing the operation of the device

B. Fusion-specific Requirements for Hall Sensors

Two-dimensional Hall arrays have been used outside of fusion in educational tools [10], consumer electronics [11], non-destructive testing [12], and metallic object detection [13]. These devices all share a basic systems architecture underpinned by the use of multiplexed sensors, however these existing designs are ill-suited to operation in a fusion environment. Key requirements for operation in SOUTH include:

Sensitivity and Range: The array must measure both the strong toroidal field at approximately 100 mT and potential near-zero stray radial magnetic field components.

Bandwidth and Sampling: Given the short pulse duration of 100 ms, the array requires a high analog bandwidth and associated sampling rate. A bandwidth exceeding 10 kHz — the PWM switching speed of SOUTH’s power supplies — is desirable.

Miniaturization: The array must fit within the vacuum vessels via its standard flanges with a maximum width of 150 mm, while still covering the plasma boundary region of interest.

Environmental: The array must maintain a low noise floor (in order to achieve the desired sensitivity) and resist environmental noise sources, including switching transients and RF interference, particularly around the ISM band at 13.56 MHz.

II. DEVICE DESCRIPTION & METHODOLOGY

The final device works by simultaneously sampling a large number of sensors using two discrete ADCs, minimizing the multiplexing requirements. The analog and digital electronics are physically separated, allowing the analog board to fit inside the vacuum vessel. This modular design also supports multiple digital processing configurations, design for different use cases.

A. Analog Electronics

The selected Hall sensor is the Texas Instruments DRV5055A4, which supports a measurement range up to ± 179 mT when powered at 3.3 V and offers an analog bandwidth of 20 kHz [14]. The sensors outputs a voltage

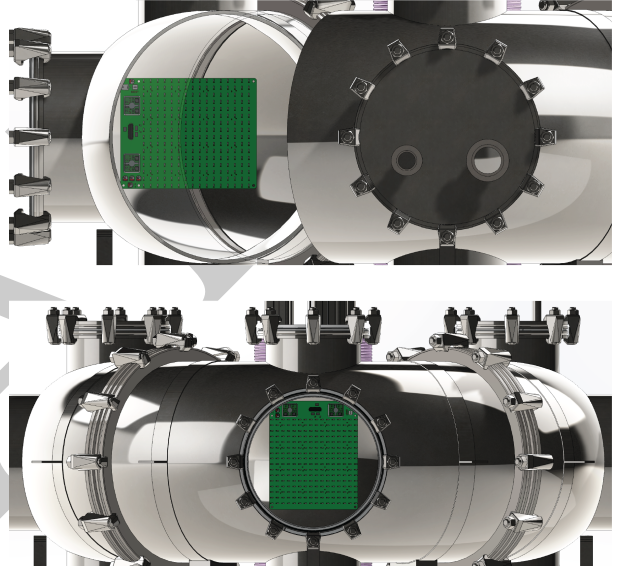


Fig. 3. Positioning of the tile within SOUTH. The top configuration monitors toroidal magnetic field while the bottom configuration monitors radial component. The device could also be positioned facing upwards to measure the poloidal field.

proportional to the magnetic field ($V \propto B$), with zero field corresponding to $V_{CC}/2$. This architecture enables all 256 sensors to share a common reference with both ADCs, ensures that all voltages remain within the linear region of all operational op-amps, and provides some common-mode immunity from noise.

Sensor outputs are routed through a high-performance analog multiplexer, buffered by a low-noise rail-to-rail op-amp, and through a single-stage Sallen-key low-pass filter, before being buffered again by an ADC driver and digitized. The filter’s pole frequency f_p is tuned to allow five time constants of settling at a sampling rate of 40 kSPS after accounting for the increased sampling rate required for the multiplexing. This filter mitigates high-frequency switching noise and RF interference but does not serve as an anti-aliasing filter. Consequently, the system is susceptible to aliasing from interference in the 20–1000 kHz range. The inability to implement effect

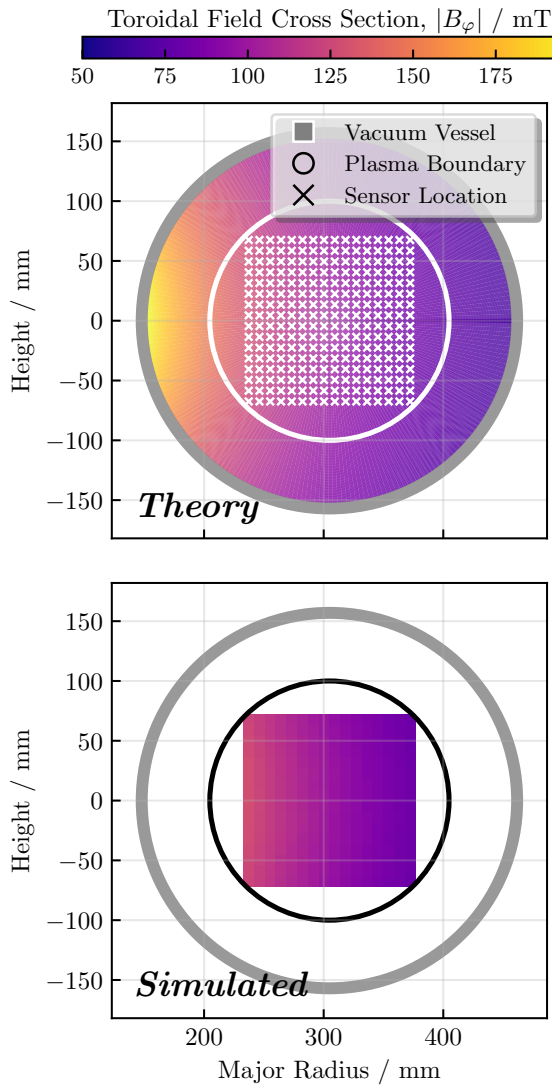


Fig. 4. Idealized experimental setup within SOUTH showing sensor geometry and expected field strength, and simulated reconstruction of the toroidal field B_ϕ including simulated noise based on the results shown in Figure 6

anti-aliasing without incurring significant cost is the primary limitation of the multiplexed topology.

The chosen ADC is a 12-bit, simultaneously sampling, successive-approximation register part, featuring four ADCs on a shared silicon multiplexed to eight inputs with a shared digital controller. Each ADC has its own quad-SPI bus capable of clocking out samples as fast as 4 MSPS per ADC (for 16 MSPS total) [15]. In addition to the aforementioned common-mode immunity, both the ADCs and ADC driver are shielded from potential interference inside mu-metal enclosures.

Due to the analog electronics' reliance on the power rail for both supply and a reference voltage, a low-noise linear dropout regulator (LDO) is used to provide an extremely stable 3.3 V common-carrier voltage from an input voltage in the range of 4–5 V. This high-precision analog configuration is designed to achieve sub-mT resolution across a dynamic range exceeding 150 mT.

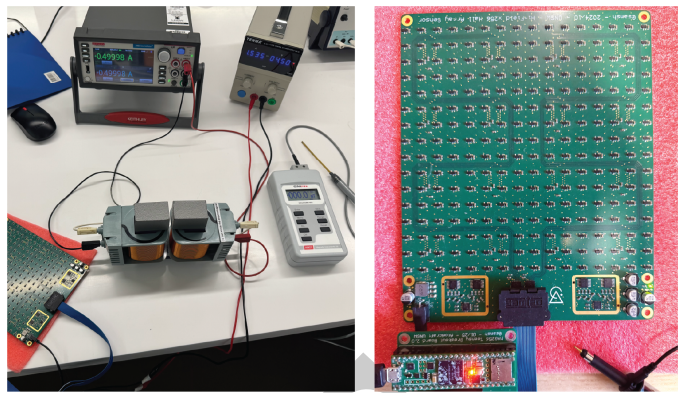


Fig. 5. Linearity calibration setup with source meter, gauss meter, and ferrite core electromagnet (left), and close-up of the completed device (right) with the Teensy digital controller board.

B. Digital Electronics

The compact dimensions inside SOUTH's vacuum vessel necessitate a separate digital control assembly. The main analog PCB includes three buffer/level shifter ICs which enable operation with both 3.3 V and 1.6 V logic, allowing interfacing with a wide range of controllers over a standard, high-performance SYZYGY FPGA connector. So far two compatible digital halves have been designed: one for user-friendly, interactive operation using a microcontroller, and another for high-performance data acquisition using an FPGA.

The microcontroller-based solution uses a Teensy 4.1 [16] and is capable of sampling at up to 6 kSPS using dual hardware SPI interfaces. The Teensy can support 25 MHz one-wire SPI, but can achieve 48 MHz with reduced stability. In this configuration, the ADC's build-in hardware oversampling is used to reduce bandwidth and mitigate aliasing, while also decreasing the data volume. Full-rate sampling is not feasible due to bus speed and memory limitations.

The FPGA implementation uses a Pynq Z2 FPGA development board, capable of exceeding the 40 kSPS Nyquist frequency required for the 20 kHz sensors bandwidth. This is achieved using two four-wire SPI interfaces in parallel at bus speeds exceeding 50 MHz. The FPGA configuration is intended for high-performance, triggered measurements, though real-time interaction has been demonstrated as possible by other groups [12] and could be developed in future,

C. Data Processing & Analysis

To convert raw ACS output codes into meaningful images, each code is mapped to a spatial location in two dimensions, then converted to a voltage and a magnetic field using the sensor sensitivity and DC offset. This processing is performed externally on a host computer. For the FPGA-based implementations, additional processing is required to apply a phase correction to each sensors fully reconstructed (with $\sin x/x$ interpolation) analogue waveforms to correct for rolling-shutter effects that are an inevitable consequence of the multiplexed topology. For real-time operations, the acquisition rate is significantly faster than the display refresh rate, rendering rolling shutter effects negligible.

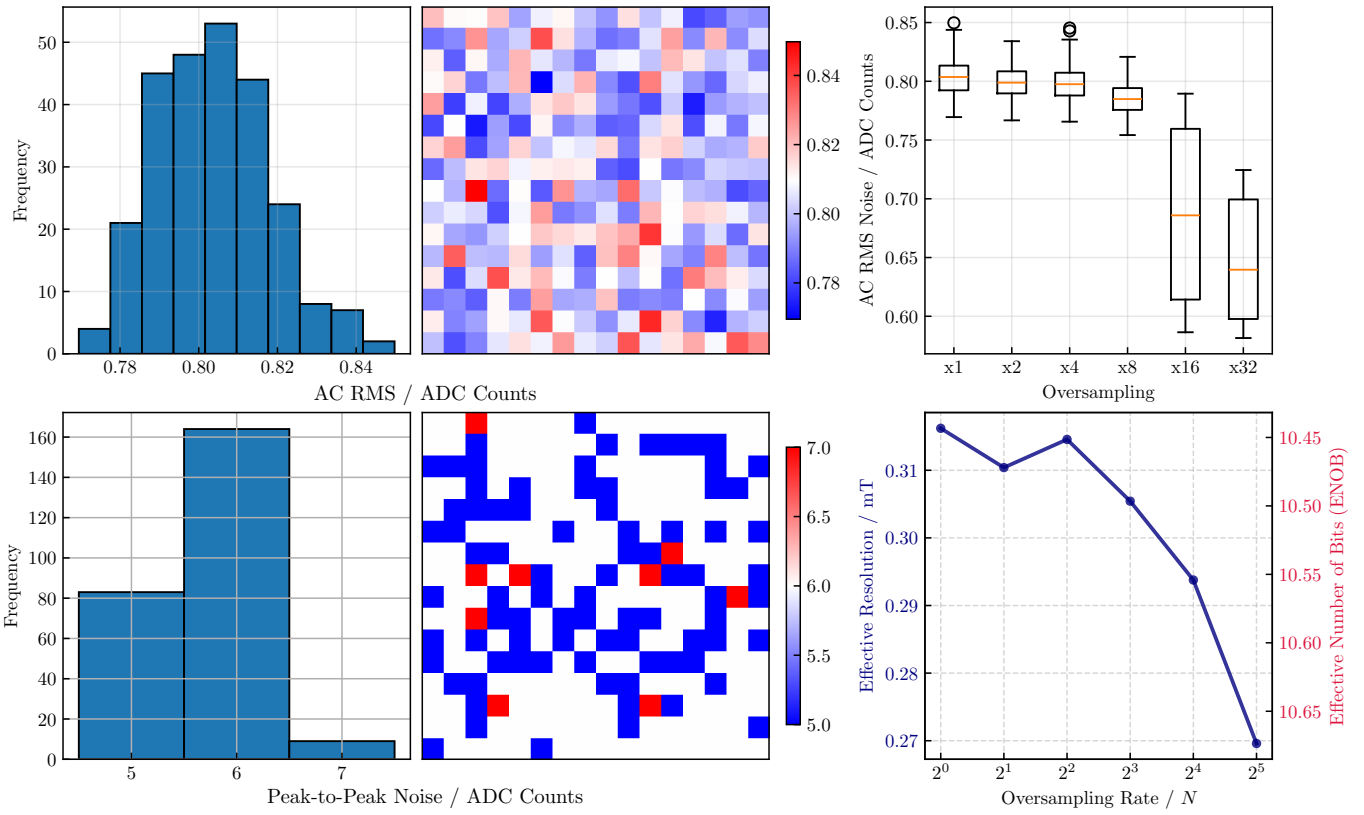


Fig. 6. Peak-to-peak and AC RMS noise data, spatial distributions, and effective resolution as a function of hardware oversampling window size.

Bicubic interpolation between adjacent sensors has been employed in previous Hall array implementations [11], [12], and is used here in post-processing where its computational cost is negligible. Figure 7 presents selected results enhanced via bicubic interpolation; this method is effective when the spatial resolution of the sensor array exceeds the granularity of the magnetic field being reconstructed, such as in the case of the tokamak's toroidal field cross-section, but localized field — such as those generated by small button magnets — are vulnerable to artifacting.

D. Use in SOUTH Tokamak

The primary application of the device in the SOUTH tokamak is to validate the magnitude and spatial configuration of the toroidal field. Figure 4 illustrates the theoretically ideal toroidal field, alongside a simulated reconstruction incorporating modeled device noise. The imaging capability of the array is expected to confirm the characteristic $B_\varphi \sim 1/R$ relationship and allow comparison with multiphysics simulations. The device could also potentially offer some quantitative measurement of magnetic field ripple.

A secondary application involves monitoring the radial magnetic field, which should ideally be 0 at the center of the toroidal field. Deviations from this expectation would indicate the presence of stray magnetic fields, and this would in turn indicate issues with the magnetic field system that could be flagged for further investigation. Since each sensor measures the field component parallel to its normal vector, the array

must be positioned to intersect the field lines of interest, as shown in Figure 3.

III. PRELIMINARY RESULTS

The device functions generally well; the microcontroller setup is capable of much faster sampling than anticipated, making the FPGA implementation unnecessary except for when the full 20 kHz bandwidth is required. Interactive plotting in real time also works reliably, and data can be logged at up to 1000 times per second easily on a laptop, using the most stable clock configurations with oversampling.

Some preliminary static imagery is shown in Figure 7, but the device's functionality is best demonstrated more interactively as in the videos contained in the supporting materials.

A. Quantification of Noise

Measurements of noise were conducted in zero magnetic field, over a sampling period of 10,000 samples collected with a filter settling time representative of maximum speed operation. As shown in Figure 6, all 256 sensors perform generally similarly and there is no significant geometric correlation of noise statistics between adjacent sensors or sensors that share a filtering circuit or ADC. The device demonstrates a very low AC RMS noise floor below one least-significant bit, and a correspondingly excellent effective resolution of well under 1 mT. The noise statistics do not drop off as expected with the introduction of hardware oversampling, likely because the

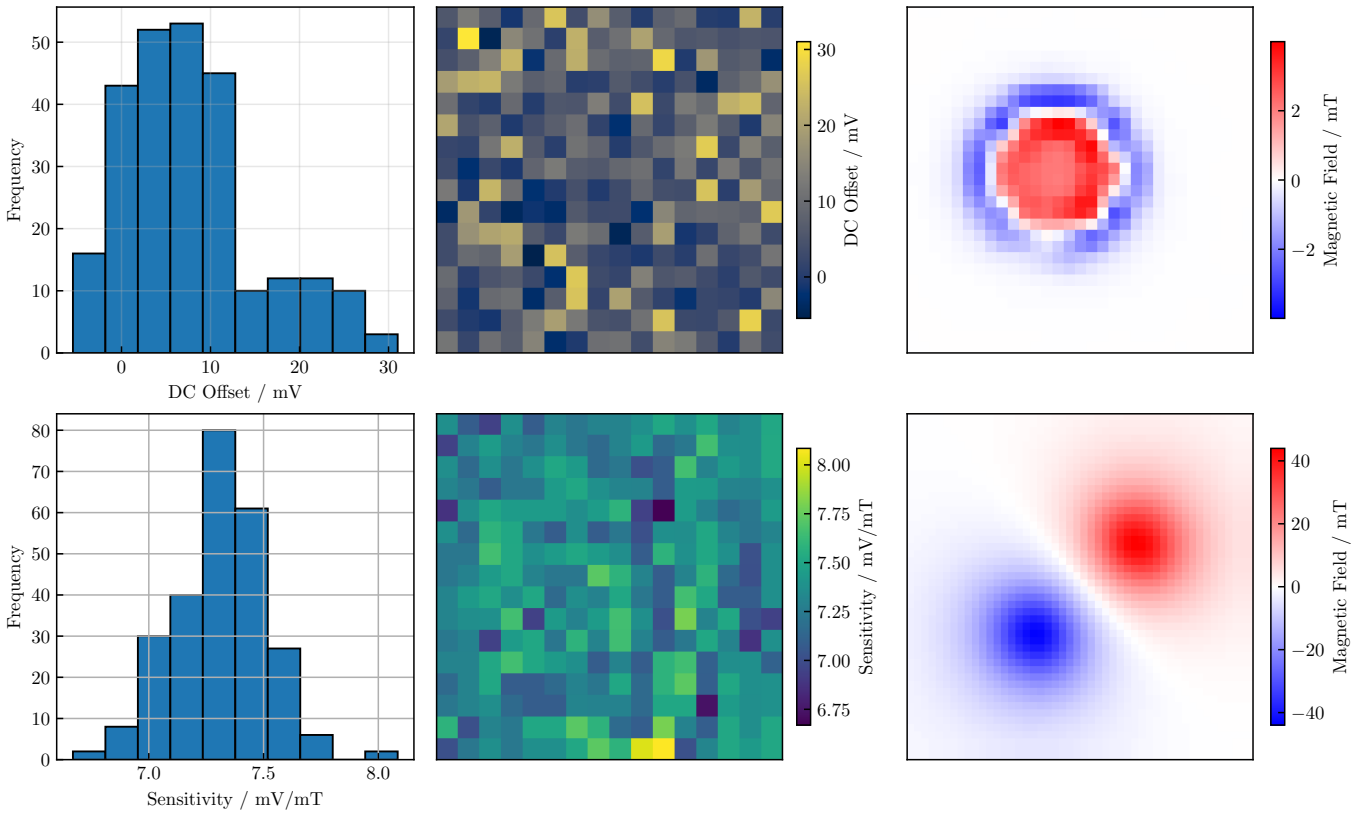


Fig. 7. Calibration results — showing the DC offset of a zero field (top) and the linear magnetic field sensitivity (bottom) — and preliminary imagery (right) of an Apple MagSafe charger and a very strong bar magnet, showing the use of bicubic interpolation. The manufacturer quotes an expected sensitivity of 7.5 mV/mT [14].

noise floor is dominated by quantization noise. This indicates that future iterations could benefit from the use of higher-resolution ADCs.

B. Calibration

The DC offset at zero field compared to the accepted value was determined through the averaging of several thousands of measurements, as shown in Figure 7. The calibration of linearity was done using a ferrite-core electromagnet powered by a source-measure unit to produce an extremely constant and uniform magnet field, which was first measured with a four-digit gaussmeter before every sensor on the PCB took both a positive and negative measurement of an approximately 115 mT magnetic field, with variations across the magnet cross section of under 1 %. Both the linearity and DC offset constant showed no noticeable geometric correlation.

IV. DISCUSSIONS & FUTURE WORK

The scope of the 2D Hall array in this configuration is inherently limited to small, spherical tokamaks where the array dimensions can be reasonably compared to the toroidal region of interest while maintaining sufficient sensor granularity. This device offers small fusion endeavors a cost-effective alternative to the comprehensive field mapping solutions available to larger, more mature projects.

The device demonstrates significant pedagogical potential, serving as digital version of magnetic viewing film. It could enhance undergraduate instruction in general physics and introductory electromagnetism courses by enabling direct observation of fundamental concepts, like the magnetic fields produced by current-carrying wires. The visual and interactive nature of the device makes it particularly suitable for outreach activities, and *AtomCraft* will use it to attract new students recruits.

This device also represents the current practical limit of what can be achieved with off-the-shelf technologies. Custom Hall sensors could provide increased analog bandwidth and field range, but only at significantly higher cost and with much added complexity. The low observed noise floor should give future projects confidence to invest in higher resolution ADCs to increase dynamic range, though the utility of higher resolutions is questionable. Future work could focus on turning this array into a plasma diagnostic, potentially targeting a poloidal application similar to what was demonstrated in [9].

A. Conclusion

This paper has presented the design, performance, and preliminary results of a high-resolution 2D Hall effect array device built to aid in the research and development of a small spherical tokamak. By functioning as a magnetic field camera, the arrays can image the toroidal fields within the region

of plasma confinement and de-risk engineering efforts by verifying that generated magnetic fields match multiphysics simulations.

The demonstrated system provides a practical, cost-effective solution for magnetic field mapping in resource-constrained environments while offering substantial educational value. The low noise performance achieved with commercial components establishes a new benchmark for future developments of similar systems, in fusion engineering and beyond.

SUPPORTING MATERIAL

Please see the attached supporting materials for video demonstrations of the device in action (alternatively, view on YouTube here and here). Detailed schematics, manufacturing documents and analysis software can be made available on request to the corresponding author.

ACKNOWLEDGMENT

We would like to thank all the students and academics of AtomCraft — especially Patrick Burr and Ed Obbard — for providing the context for this research, as well as enabling our access to facilities. Thank you to the lab staff in the mechatronics research laboratory and physics higher-years teaching laboratory for the use of their facilities and guidance.

REFERENCES

- [1] AtomCraft collaboration, private internal communications, 2024–2025.
- [2] S. K. Nielsen et al., “First results from the NORTH tokamak,” *Fusion Engineering and Design*, vol. 166, p. 112288, May 2021, doi: 10.1016/j.fusengdes.2021.112288.
- [3] A. Sykes et al., “The ST25 Tokamak for rapid technological development,” in *2013 IEEE 25th Symposium on Fusion Engineering (SOFE)*, Jun. 2013, pp. 1–4. doi: 10.1109/SOFE.2013.6635330.
- [4] M. Agredano-Torres et al., “Coils and power supplies design for the SMART tokamak,” *Fusion Engineering and Design*, vol. 168, p. 112683, Jul. 2021, doi: 10.1016/j.fusengdes.2021.112683.
- [5] M. Hasegawa et al., “Current status and prospect of plasma control system for steady-state operation on QUEST,” *Fusion Engineering and Design*, vol. 112, pp. 699–702, Nov. 2016, doi: 10.1016/j.fusengdes.2016.04.016.
- [6] R. Chavan et al., “The magnetics diagnostic set for ITER,” *Fusion Engineering and Design*, vol. 84, no. 2, pp. 295–299, Jun. 2009, doi: 10.1016/j.fusengdes.2008.12.103.
- [7] X. Wu, H. Huang, L. Peng, Y. Huang, and Y. Wang, “Algorithm Research on the Conductor Eccentricity of a Circular Dot Matrix Hall High Current Sensor for ITER,” *IEEE Transactions on Plasma Science*, vol. 50, no. 6, pp. 1962–1970, Jun. 2022, doi: 10.1109/TPS.2022.3173286.
- [8] N. Marconato, E. Sartori, and G. Serianni, “Numerical and Experimental Assessment of the New Magnetic Field Configuration in SPIDER,” *IEEE Transactions on Plasma Science*, vol. 50, no. 11, pp. 3884–3889, Nov. 2022, doi: 10.1109/TPS.2022.3167859.
- [9] B. A. Stevenson, S. F. Knowlton, G. J. Hartwell, J. D. Hanson, and D. A. Maurer, “Hall probe measurements of the poloidal magnetic field in Compact Toroidal Hybrid plasmas,” *Review of Scientific Instruments*, vol. 85, no. 9, p. 093502, Sep. 2014, doi: 10.1063/1.4894209.
- [10] P. Jansen, “A Third, High-Speed Magnetic Imager Tile,” *Hackerday.io*. Accessed: Nov., 2024. [Online]. Available: <https://hackaday.io/project/18518-iteration-8/log/91551-a-third-high-speed-magnetic-imager-tile>
- [11] R. H. Liang, K. Y. Cheng, C. H. Su, C. T. Weng, B. Y. Chen, and D. N. Yang, “Gausssense: attachable stylus sensing using magnetic sensor grid,” in *Proceedings of the 25th annual ACM Symposium on User Interface Software and Technology*, Cambridge, MA, Oct. 2012. doi: 10.1145/2380116.2380157.
- [12] C.-W. Liang, E. Balaban, E. Ahmad, Z. Zhang, J. Sexton, and M. Missous, “A real time high sensitivity high spatial resolution quantum well hall effect magnetovision camera,” *Sensors and Actuators A: Physical*, vol. 265, pp. 127–137, 01 2017, doi: 10.1016/j.sna.2017.08.035.
- [13] J. Cai, T. Zhou, Y. Xu, and X. Zhu, “A High-Resolution Magnetic Field Imaging System Based on the Unpackaged Hall Element Array,” *Applied Sciences*, vol. 14, no. 13, Art. no. 13, Jan. 2024, doi: 10.3390/app14135788.
- [14] Texas Instruments, “Ratiometric Linear Hall Effect Sensor,” DRV5055 datasheet, Jan. 2018 [Revised Apr. 2021].
- [15] Analog Devices, “Single-Ended Input, Quad, Simultaneous Sampling, 16-Bit/14-Bit/12-Bit, SAR ADC,” AD7386-4/AD7387-4/AD7388-4 datasheet, Oct. 2023.
- [16] P. Stoffregen, “Teensy 4.1 Development Board,” PJRC, 2020. [Online]. Available: <https://www.pjrc.com/store/teensy41.html>

Samuel Shelton placeholder text.



Will Midgley placeholder text. Both biographies combined take up just under half a column of text.

